Flat Plate Hydrofoil

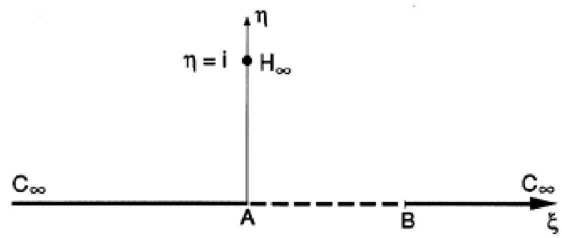

Figure 1: The ζ-plane for the linearized theory of a partially cavitating flat plate hydrofoil.

The algebra associated with the linear solutions for a flat plate hydrofoil is fairly simple, so we will review and examine the results for the supercavitating foil (Tulin 1953) and for the partially cavitating foil (Acosta 1955). Starting with the latter, the z-plane is shown on the left in the figure in section (Nug), and this can be mapped into the upper half of the ζ-plane in Figure 1 by

$$\zeta = i\left(1 + \frac{1}{z-1}\right)^{\frac{1}{2}} \qquad \text{(Nuh1)}$$

The point H_∞ at $\eta = i$ corresponds to the point at infinity in the z-plane and the point C_∞, the trailing edge of the foil, is the point at infinity in the ζ-plane. It follows that the point B, the cavity closure point, is at $\xi = c$ where $c = (\ell/(1-\ell))^{1/2}$ and ℓ is the length of the cavity, AB, in the physical plane. The chord of the hydrofoil, AC, has been set to unity. Since there must be square-root singularities at A and B, since v is zero on the real axis in the intervals $\xi < 0$ and $\xi > c$ and $u' = \sigma U_\infty/2$ in $0 < \xi < c$, and since w must be everywhere bounded, the general form of the solution may be written down by inspection:

$$w(\zeta) = \frac{\sigma U_\infty}{2} + \frac{U_\infty(C_0 + C_1\zeta)}{[\zeta(\zeta - c)]^{1/2}} \qquad \text{(Nuh2)}$$

where C_0 and C_1 are constants to be determined. The Kutta condition at the trailing edge, C_∞, requires that the velocity be finite and continous at that point, and this is satisfied provided there are no terms of order ζ^2 or higher in the series $C_0 + C_1\zeta$.

The conditions that remain to be applied are those at the point of infinity in the physical plane, $\eta = i$. The nature of the solution near this point should therefore be examined by expanding in powers of $1/z$. Since $\zeta \rightarrow i + i/2z + O(z^{-2})$ and since we must have that $w \rightarrow -i\alpha U_\infty$, expanding Equation (**??**) in powers of $1/z$ allows evaluation of the real constants, C_0 and C_1, in terms of α and σ:

$$C_0 = \beta_1\alpha + \beta_2\sigma/2 \quad ; \quad C_1 = \beta_2\alpha - \beta_1\sigma/2 \qquad \text{(Nuh3)}$$

where

$$\beta_1, \beta_2 = \left[\frac{1}{2}\left\{(1-\ell)^{-1/2} \pm 1\right\}\right]^{\frac{1}{2}} \qquad \text{(Nuh4)}$$

In addition, the expansion of w in powers of $1/z$ must satisfy the last equation of section (Nue). If the cavity is finite, then $Q = 0$ and evaluation of the real part of the coefficient of $1/z$ leads to

$$\frac{\sigma}{2\alpha} = \frac{2 - \ell + 2(1-\ell)^{\frac{1}{2}}}{\ell^{\frac{1}{2}}(1-\ell)^{\frac{1}{2}}} \tag{Nuh5}$$

while the imaginary part of the coefficient of $1/z$ allows the circulation around the foil to be determined. This yields the lift coefficient,

$$C_L = \pi\alpha \left[1 + (1-\ell)^{-\frac{1}{2}}\right] \tag{Nuh6}$$

Thus the solution has been obtained in terms of the parameter, ℓ, the ratio of the cavity length to the chord. For a given value of ℓ and a given angle of attack, α, the corresponding cavitation number follows from equation (Nuh5) and the lift coefficient from equation (Nuh6). Note that as $\ell \to 0$ the value of C_L tends to the theoretical value for a noncavitating flat plate, $2\pi\alpha$. Also note that the lift-slope, $dC_L/d\alpha$, tends to infinity when $\ell = 3/4$.

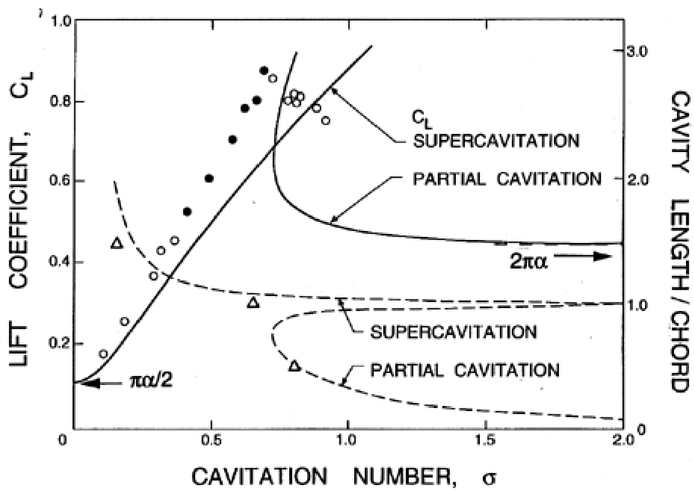

Figure 2: Typical results from the linearized theories for a cavitating flat plate at an angle of attack of 4°. The lift coefficients, C_L (solid lines), and the ratios of cavity length to chord, ℓ (dashed lines), are from the supercavitation theory of Tulin (1953) and the partial cavitation theory of Acosta (1955). Also shown are the experimental results of Wade and Acosta (1966) for ℓ ($\triangle$) and for C_L ($\circ$ and $\bullet$) where the open symbols represent points of stable operation and the solid symbols denote points of unstable cavity operation.

In the supercavitating case, Tulin's (1953) solution yields the following results in place of equations (Nuh5) and (Nuh6):

$$\alpha\left(\frac{2}{\sigma} + 1\right) = (\ell - 1)^{\frac{1}{2}} \tag{Nuh7}$$

$$C_L = \pi\alpha\ell\left[\ell^{\frac{1}{2}}(\ell-1)^{-\frac{1}{2}} - 1\right] \tag{Nuh8}$$

where now, of course, $\ell > 1$. Note that the lift-slope, $dC_L/d\alpha$, is zero at $\ell = 4/3$.

The lift coefficient and the cavity length from equations (Nuh5) to (Nuh8) are plotted against cavitation number in Figure 2 for a typical angle of attack of $\alpha = 4°$. Note that as $\sigma \to \infty$ the fully wetted lift coefficient, $2\pi\alpha$, is recovered from the partial cavitation solution, and that as $\sigma \to 0$ the lift coefficient tends to $\pi\alpha/2$. Notice also that both the solutions become pathological when the length of the cavity approaches the chord length ($\ell \to 1$). However, if some small portion of each curve close to $\ell = 1$ is

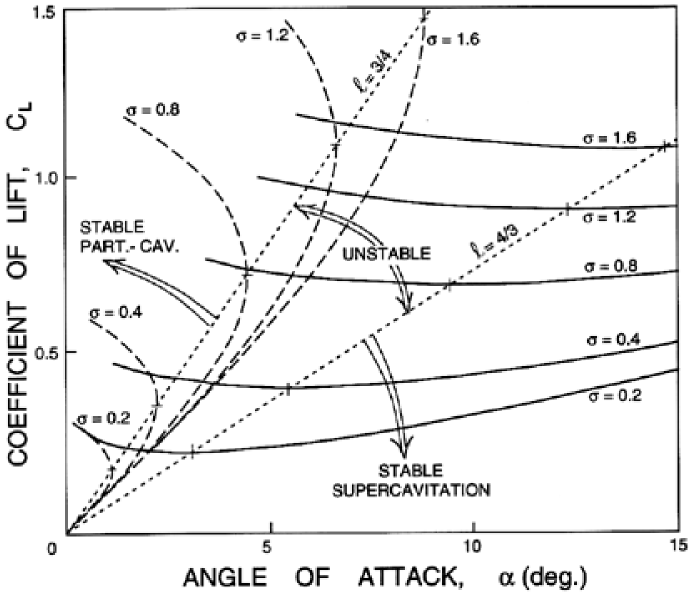

Figure 3: The lift coefficient for a flat plate from the partial cavitation model of Acosta (1955) (dashed lines) and the supercavitation model of Tulin (1953) (solid lines) as a function of angle of attack, α, for several cavitation numbers, σ, as shown. The dotted lines are the boundaries of the region in which the cavity length is between 3/4 and 4/3 of a chord and in which $dC_L/d\alpha < 0$.

eliminated, then the characteristic decline in the performance of the hydrofoil as the cavitation number is decreased can be observed. Specifically, it is seen that the decline in the lift coefficient begins when σ falls below about 0.7 for the flat plate at an angle of attack of 4°. Close to $\sigma = 0.7$, one observes a small increase in C_L before the decline sets in, and this phenomenon is often observed in practice, as illustrated by the experimental data of Wade and Acosta (1966) included in Figure 2.

The variation in the lift with angle of attack (for a fixed cavitation number) is presented in Figure 3. Also shown in this figure are the lines of $\ell = 4/3$ in the supercavitation solution and $\ell = 3/4$ in the partial cavitation solution. Note that these lines separate regions for which $dC_L/d\alpha > 0$ from those for which $dC_L/d\alpha < 0$. Heuristically it could be argued that $dC_L/d\alpha < 0$ implies an unstable flow and the corresponding region in figure 3 for which $3/4 < \ell < 4/3$ does, indeed, correspond quite closely to the observed regime of unstable cavity oscillation (Wade and Acosta 1966).